2302
doi:10.1017/S1431927622008844
Microsc. Microanal. 28 (Suppl 1), 2022

Orientation-Specific CDW Phase Transition Temperatures in 1*T*-TaS_2

Paige E. Engen[1,2] and David J. Flannigan[1,2*]

[1.] Department of Chemical Engineering and Materials Science, University of Minnesota, Minneapolis, MN, USA.
[2.] Minnesota Institute for Ultrafast Science, University of Minnesota, Minneapolis, MN, USA.
* Corresponding Author: flan0067@umn.edu

The metastable 1*T* structure of TaS_2 displays a rich set of structural and electronic phases. Owing to sensitivity of these phases to *local* structural inhomogeneities, selected-area studies of temperature-dependent nanoscale behaviors may reveal new and unexpected behaviors. Here, we describe our observation of slight, spatially dependent variations in transition temperatures for structurally degenerate layer stacking arrangements in multilayer 1*T*-TaS_2 crystals. In general, the 1*T* structure supports an incommensurate (IC), a nearly commensurate (NC), and a commensurate charge-density-wave (CDW) phase. Small amplitude distortions lacking long-range order constitute the IC phase. Upon cooling, the distortions coarsen and form an uncommon NC phase comprised of commensurate domains of CDW groupings separated by discommensurations. Further cooling produces the fully commensurate C phase. Reference vectors defining the CDW superlattice orientation in the NC phase are rotated by $\varphi = \pm 13.9°$ relative to a low-index direction in the undistorted crystal lattice. This angle decreases with increasing temperature until the IC phase dominates the overall structure. Owing to the nature of the CDW layer stacking, combinations of the superlattice rotations and stacking orientations result in four degenerate NC phases and two degenerate IC phases (Fig. 1a). SAED patterns from thin, single-crystal specimens contain six first-order CDW satellite spots that alternate between $\pm 1/3\mathbf{c^*}$ azimuthally around the Bragg spot, and six second-order satellite spots arising from basal plane structure. Thus, CDW phases and orientations can be identified and quantified by analyzing the patterns. However, the precise ordering and the nature of phases within such specimens can contain multiple regions of varying CDW orientations. Indeed, coexisting degenerate NC-phase orientations are common and can be manipulated with optical pulses [1], and structural heterogeneities and strain can alter transition temperatures [2-4]. Such effects have local origins, as has been indicated with *in situ* TEM heating experiments that track diffusion-driven transformation fronts [5]. Importantly, such behaviors suggest discrete, *local* domains may display slight variations in transition temperatures, suggesting an extremely sensitive dependence of the CDW potential energy landscape on subtle structural modulations.

To explore sensitivities of transition temperatures to local structures, we conducted *in situ* TEM thermal cycling experiments on 1*T*-TaS_2 flakes cut from bulk crystals using an ultramicrotome. SAED patterns were collected approximately along the [001] direction and at temperatures ranging from 300 to 370 K (*i.e.*, spanning the NC-IC transition; Fig. 1b-e). Near the transition points, patterns were collected every 2 K once thermal equilibration had been reached at each step. Starting with the NC phase (Fig. 1b), heating induces the first-order spots to rotate, indicative of commencement of the transition to the IC phase (Fig. 1c). Further slight heating causes the second-order spots to rotate, representing a complete transition to the IC phase (Fig. 1d,e). Interestingly, we observed a difference of 2 K in the NC to IC transition temperature for the first-order and second-order satellite spots (which we call the Type A transition). Closer examination shows the same 2 K difference in transition temperature for adjacent first-order spots (Type B transition; Fig. 1f). Tilting away from the [001] zone axis confirms the presence of two degenerate stacking orientations based on the ordering of first-order spots located at

±1/3**c*** (Fig. 1g). Diffraction patterns obtained from regions with both stacking orientations display all six first-order spots located at ±1/3**c***; adjacent spots result from CDWs with different orientations. Note that because the IC second-order spots have a much lower intensity than the NC-phase satellite spots, a significant fraction of the region of interest must consist of IC phase domains in order to track the phase transition with second-order spots. This means that while both the NC and IC phases contribute to the second-order spots during the Type A transition, the intensity difference is too large to observe. Thus, stepwise with heating, the Type A state first transitions to the IC phase, while the second-order spots arise only from the NC phase. Next, the Type B transition begins to be dominated by the IC phase, while the second-order spots arise from both the NC and IC phases. Finally, the entire field of view fully transitions to the IC phase (Fig. 1h). Accordingly, we have found that CDW stacking orientations can have display slightly varied transition temperatures, potentially arising from distinct structural features within individual domains. Indeed, higher defect densities and strain generally lead to reduced transition temperatures upon heating [2, 4], but additional work is required to determine the precise, atomic-scale origins of the subtle, spatially-dependent variations observed here [6].

https://doi.org/10.1017/S1431927622008844 Published online by Cambridge University Press

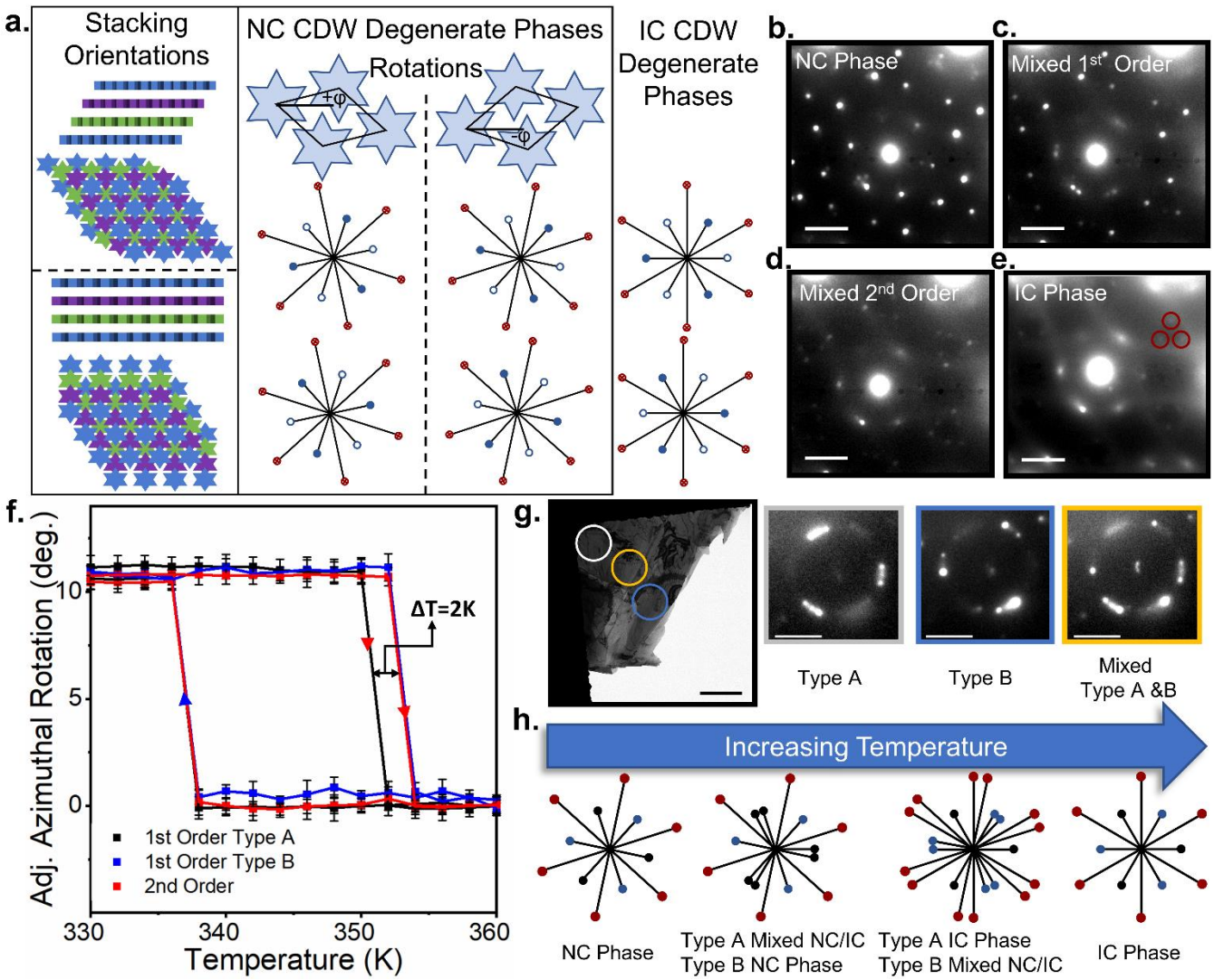

Figure 1: Orientation-specific CDW phase transitions in 1*T*-TaS_2 (a) Schematic of the different degenerate TaS_2 CDW layer stacking configurations, CDW orientations, and resulting reciprocal-space scattering patterns for the NC and IC phases. The Stars of David represent the CDW distortion. Side and plain views for the ABC repeat (blue, purple, green) stacking arrangement are shown. φ is the rotation angle for the √13**a** superlattice. Surrounding the Bragg spots (black) are the first-order satellites (open blue = -1/3**c***, solid blue = +1/3**c***) and the second-order satellites (red, in the basal plane). (b-e) Diffraction patterns arising from (b) the NC phase, (c) mixed NC-IC domains showing first-order spots, (d) mixed NC-IC domains showing second-order spots, and (e) the IC phase. Red circles highlight a set of second-order spots. (f) Relative azimuthal rotation for the CDW spots from 330 to 360 K at 2-K steps (fully equilibrated at each step). The Type A (black), Type B (blue), and 2nd order data (red) are the average of 10, 3, and 5 spots, respectively. Error bars are one standard deviation of the average. Arrows show the direction of heating (red) and cooling (blue). (g) Bright-field image (scale bar = 5 µm) and SAEDs (white = Type A, yellow = mixed, and blue = Type B) showing different CDW orientations. (h) Reciprocal-space scattering schematics, with black = Type A, at +1/3**c***; blue = Type B, at +1/3**c***; and red = second-order, basal plane. All diffraction pattern scale bars = 1 nm^{-1}.

https://doi.org/10.1017/S1431927622008844 Published online by Cambridge University Press

References:

[1] A Zong et al., Sci. Adv. **4** (2018), p. eaau5501.
[2] H Mutka et al., Radiat. Eff. **45** (1980), p. 219.
[3] AW Tsen et al., Proc. Nat. Acad. Sci. U.S.A. **112** (2015), p. 15054.
[4] R Zhao et al., Nano Lett. **17** (2017), p. 3471.
[5] J Van Landuyt et al., Phys. Status Solidi A **42** (1977), p. 565.
[6] This material is based upon work supported by the National Science Foundation under Grant No. DMR-1654318. Acknowledgment is made to the Donors of the American Chemical Society Petroleum Research Fund for partial support of this research under Award No. 60584-ND10. This material is based upon work supported by the National Science Foundation Graduate Research Fellowship Program under Grant No. DGE-1839286.

https://doi.org/10.1017/S1431927622008844 Published online by Cambridge University Press